ACS OMEGA

Article

Cite This: ACS Omega 2019, 4, 14092−14099

http://pubs.acs.org/journal/acsodf

Dose-Dependent Efficacy of Gold Clusters on Rheumatoid Arthritis Therapy

Qing Yuan,[†,‡,⊥] Yao Zhao,[§,⊥] Pengju Cai,[§] Zhesheng He,[§] Fuping Gao,[*,§] Jinsong Zhang,[∥] and Xueyun Gao[*,†,‡,§]

[†]Department of Chemistry and Chemical Engineering, Beijing University of Technology, Beijing 100124, China

[‡]Center of Excellence for Environmental Safety and Biological Effects, Beijing University of Technology, Beijing 100124, China

[§]CAS Key Laboratory for the Biological Effects of Nanomaterials and Nanosafety, Institute of High Energy Physics, Chinese Academy of Sciences, Beijing 100049, China

[∥]Key Laboratory of Tea Biochemistry & Biotechnology, School of Tea and Food Science, Anhui Agricultural University, Hefei 230036, Anhui, PR China

ABSTRACT: Chronic inflammation and progressive bone damage in joints are two main pathological features of rheumatoid arthritis (RA). We have synthesized a gold cluster with glutathione ($Au_{29}SG_{27}$) (named GA) that can effectively suppress both inflammation and bone damage in collagen-induced arthritis (CIA) in rats. Thus, gold clusters showed great potential for the therapy of RA. However, the optimal therapeutic dose remaining has to be determined. Therapeutic effect and safety are largely relying on drug dosage. Specifying the dose-dependent effects of GA on both therapy and biosafety can facilitate its clinical transformation research. Therefore, in this study, we comprehensively evaluated the dose-dependent efficacy of GA on the 30-day toxicity and RA treatment in rats. Results showed that continuous intraperitoneal injection of GA at a dose of 15 mg/kg (Au content) for 30 days resulted in slight hematological abnormalities and increases on organ coefficients of kidney and adrenal gland, while 10 mg Au/kg did not cause any obvious toxicity and side effects. In the treatment of CIA rats, only when the dose of GA reached 5 mg Au/kg, the symptoms of RA could be significantly improved. With regard to the histopathological analysis, although a lower dose of GA can suppress inflammation and bone damage to some extent, only the 5 mg Au/kg treatment could restore them to a state close to the normal control group. Therefore, we infer that 5 mg Au/kg is the optimal dose of GA for RA therapy in rats, which provides a theoretical basis for further preclinical research.

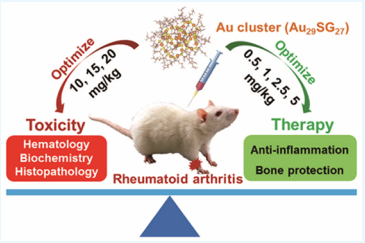

INTRODUCTION

Rheumatoid arthritis (RA) is one of the most common autoimmune and chronic inflammatory diseases, afflicts about 0.5 to 1% of the world's population.[1,2] Chronic synovial inflammation and progressive cartilage/bone destruction in joints are two major pathologic features of RA.[2] Bone erosion is the major cause of disability that severely reduces the life quality of patients, carrying a tremendous burden for both the individual and society.[1,3] Despite that a therapeutic revolution for RA treatment in the past decade has improved the disease outcomes, there is still many patients who do not respond to current therapies or do not benefit from them due to severe side effects.[1] Especially, there is still no established effective therapeutics for preventing joint damage in the long term.[4] Therefore, the design of novel therapy strategies to suppress inflammation and reduce joint destruction simultaneously is urgently required.

Chrysotherapy has been used to treat RA patients for more than 70 years and was considered as an important disease-modifying antirheumatic drug (DMARDs) with well-documented anti-inflammatory activity.[5−7] Moreover, some monovalent gold drugs showed potential activity on bone metabolism *in vitro*.[8] However, the non-negligible high toxicity and adverse side effects of these gold drugs led to discontinuation in up to 45% of treated patients, which resulted in a dramatic decline of chrysotherapy use in RA clinical practice.[5,9,10] Therefore, more studies are needed to develop novel gold drugs with higher activity and minimal side effects.

In recent years, Au clusters (especially the peptide-templated Au clusters) have attracted much attention for their excellent biocompatibilities and intrinsic biomedical activities.[11−14] The ease of synthesis and the unique biological properties of peptide-templated Au clusters make them ideal candidates for translation from the laboratory to the clinical use in humans.[11,15]

In a previous study, we have proven a peptide-templated Au cluster named GA ($Au_{29}SG_{27}$), which is synthesized with glutathione as the thiolate ligand and seems to be a very promising anti-arthritic formulation in RA management.[16] The Au cluster could effectively diminish the inflammation symptoms and prevent joint damage in collagen-induced

Received: July 2, 2019
Accepted: August 1, 2019
Published: August 16, 2019

DOI: 10.1021/acsomega.9b02003
ACS Omega 2019, 4, 14092−14099

arthritis (CIA) in rats, without any obvious side effects.[16] It is worth noting that the Au cluster showed more efficacy in bone protection than the clinical anchor drug for RA therapy, methotrexate. As a result, the Au cluster may provide an alternative to traditional antirheumatic drugs with more effectiveness and safety.[16,17]

Efficacy and safety are two of the most critical concerns in drug development, and there is a balance between them.[18,19] The objective of this study is to identify the optimal dose of GA, which effectively suppresses inflammation and bone damage in CIA rats, without any toxicity and side effects. The results reported in this work will be helpful to understand the not yet complete clarified toxicological and pharmacodynamic effects of gold clusters and facilitate their clinical use in the future.

RESULTS

Synthesis and Characterization of Au Clusters. The Au cluster was synthesized by using $HAuCl_4$ and glutathione (GSH) as we reported previously.[16] The GSH tripeptide was used as a thiolate ligand to anchor the produced Au clusters via strong Au−S bonds in aqueous solution, under mild conditions. The purified Au cluster was named GA and has excellent water solubility, and the aqueous solution showed a light yellow color. When excited by UV light, the solution containing GA emitted a strong red fluorescence (Figure 1A).

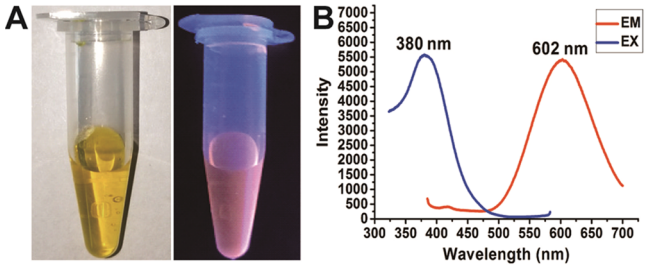

Figure 1. Characterization of the synthesized $Au_{29}SG_{27}$ cluster. (A) Photographs of the aqueous solution of $Au_{29}SG_{27}$ under (left) visible light and (right) UV light. (B) Fluorescence excitation and emission spectra of $Au_{29}SG_{27}$ (380 nm and 602 nm).

The peaks of the excitation and the emission spectra are located at 380 and 602 nm, respectively, consistent with our previous reports (Figure 1B). The precise molecular formula and structure of the Au cluster have been determined by electrospray ionization mass spectrometry and density functional theory calculations in our previous study, which can be expressed as $Au_{29}SG_{27}$.[16]

Dose-Dependent Toxicity of GA in Normal Rats. The decline in the clinical use of traditional gold drugs was due to serious side effects, which mainly include hematological toxicities (leukopenia, thrombocytopenia, and aplastic anemia) and organ damage (pulmonary, hepatitis, and kidney).[5] Therefore, biosafety of the Au cluster is our main concern in this study. Preliminarily, a 30-day toxicity assessment of the Au cluster was conducted. We found that the half lethal dose (LD_{50}) of GA injected intraperitoneally in SD rats was 288.9 ± 13 mg Au/kg.[16] According to the standard methods for measuring chronic toxicity, we choose a dose of 15 mg Au/kg as the initial assessment dose, which is about 1/20 of the LD_{50}. Simultaneously, a higher dose of 20 mg Au/kg and a lower dose of 10 mg Au/kg were chosen to assess. A control group was also set by injecting an equal volume of saline. The indicated doses of GA were intraperitoneally injected to normal male SD rats every 2 days for 30 days. In the 20 mg Au/kg treated group, one rat died after the third injection, so this dose was totally abolished. At the end of the 30-day administrate, all treated rats showed comparable body weight gains with the control group. The changes in blood parameters and organ coefficient as well as the histopathological changes of main organs were systemically evaluated. First, a routine hematological examination were performed, and the results indicated no significant difference in the hematological index compared with control rats after the treatment with 10 mg Au/kg of GA, but the 15 mg Au/kg treatment induced increases in the percentage of Gran (Gran%) and hematocrit (HCT) and decreases in the number and the percentage of Mid (Mid# and Mid%), mean corpuscular hemoglobin concentration (MCHC), and thrombocytocrit (PCT) (Table 1). In the serum biochemistry assays, no obvious change occurred in either 10 or 15 mg Au/kg GA-treated rats, compared with the control group (Table 2). Then, organ coefficients, including heart, liver, spleen, lung, kidney, testis, adrenal gland, and thymus, were calculated. Results indicated that the 15 mg Au/kg treatment increased the coefficients of the kidney and adrenal gland, while 10 mg Au/kg did not cause any significant changes in all detected organs (Table 3). Next, these organs were sectioned and stained with hematoxylin and eosin for histological examination. No notable pathological abnormalities were found in either 10 or 15 mg Au/kg treated rats (Figure 2). These results indicate that 15 mg Au/kg of GA will

Table 1. Effect of GA on Hematology of Male Rats Intraperitoneally Administrated for 30 days

groups	WBC (10^9/L)	Lymph# (10^9/L)	Mid# (10^9/L)	Gran# (10^9/L)	Lymph (%)	Mid (%)
control	3.62 ± 0.55	3.08 ± 0.50	0.39 ± 0.06	0.15 ± 0.06	87.07 ± 0.35	9.08 ± 0.96
10 mg/kg	4.01 ± 0.57	3.70 ± 0.53	0.21 ± 0.04	0.10 ± 0.01	92.21 ± 0.24	5.12 ± 0.44
15 mg/kg	3.06 ± 0.33	2.77 ± 0.33	0.15 ± 0.02[a]	0.14 ± 0.02	90.26 ± 1.37	4.85 ± 0.53[a]
groups	Gran (%)	HGB (g/L)	RBC (10^{12}/L)	HCT (L/L)	MCH (pg)	MCHC (g/L)
control	2.27 ± 0.13	142.33 ± 1.45	6.23 ± 0.19	0.39 ± 0.01	18.51 ± 0.60	354.00 ± 7.81
10 mg/kg	2.67 ± 0.32	134.60 ± 2.84	7.46 ± 0.20	0.42 ± 0.01	18.06 ± 0.25	318.81 ± 5.70
15 mg/kg	4.89 ± 0.97[a]	146.50 ± 3.93	7.90 ± 0.23	0.52 ± 0.02[a]	18.55 ± 0.28	281.47 ± 3.38[a]
groups	RDW-CV (%)	PLT (10^9/L)	MPV (fL)	PDW (%)	PCT (%)	MCV (fL)
control	20.55 ± 0.31	675.33 ± 39.96	16.49 ± 0.45	6.14 ± 0.05	0.11 ± 0.01	61.67 ± 1.88
10 mg/kg	26.04 ± 0.46	767.00 ± 72.60	18.13 ± 0.22	6.09 ± 0.01	0.14 ± 0.01	56.67 ± 0.64
15 mg/kg	20.53 ± 0.54	473.75 ± 89.94	17.10 ± 0.66	6.15 ± 0.06	0.08 ± 0.01[a]	65.93 ± 1.04

[a]Represents a significant difference compared with the control group ($p < 0.05$), $n = 5$.

DOI: 10.1021/acsomega.9b02003
ACS Omega 2019, 4, 14092−14099

Table 2. Effect of GA on Biochemistry of Male Rats Intraperitoneally Administrated for 30 days (n = 5)

groups	TBil (μM)	ALT (U/L)	AST (U/L)	TP (g/L)	urea (mM)	CR (μM)
control	1.59 ± 0.12	49.07 ± 5.15	138.33 ± 8.71	55.07 ± 2.37	7.81 ± 0.34	23.00 ± 2.52
10 mg/kg	1.39 ± 0.10	53.06 ± 2.49	87.36 ± 11.50	50.18 ± 0.57	6.71 ± 0.26	26.20 ± 2.67
15 mg/kg	1.39 ± 0.18	50.80 ± 3.03	89.80 ± 9.35	52.88 ± 1.11	7.64 ± 0.25	27.00 ± 0.71
groups	ALB (g/L)	GLOB (g/L)	A/G	GLU (mM)	TG (mM)	TC (mM)
control	24.37 ± 0.50	32.80 ± 1.82	0.70 ± 0.01	14.28 ± 1.47	0.50 ± 0.15	1.42 ± 0.10
10 mg/kg	23.72 ± 0.50	26.46 ± 0.69	0.90 ± 0.04	12.80 ± 1.26	0.50 ± 0.10	1.53 ± 0.05
15 mg/kg	24.45 ± 0.10	28.43 ± 1.17	0.87 ± 0.04	14.09 ± 0.91	0.30 ± 0.04	1.58 ± 0.06
groups	K (mM)	Na (mM)	Cl (mM)	CK (U/L)	ALP (U/L)	
control	6.77 ± 0.13	135.93 ± 0.64	95.73 ± 1.27	982.20 ± 80.23	255.30 ± 8.62	
10 mg/kg	6.33 ± 0.30	134.48 ± 0.30	95.48 ± 0.36	768.56 ± 169.42	233.10 ± 22.07	
15 mg/kg	6.80 ± 0.05	134.12 ± 1.02	96.40 ± 1.20	916.55 ± 193.20	227.50 ± 16.78	

Table 3. Effect of GA on Organ Coefficient of Rats Intraperitoneally Administrated for 30 days

groups	heart	liver	spleen	lung
control	3.680 ± 0.252	39.188 ± 2.588	2.429 ± 0.472	4.815 ± 0.197
10 mg/kg	3.605 ± 0.172	42.411 ± 0.755	2.159 ± 0.290	5.050 ± 0.239
15 mg/kg	3.612 ± 0.068	39.503 ± 0.608	2.260 ± 0.076	5.385 ± 0.128
groups	kidneys	thymus	adrenal gland	testis
control	3.774 ± 0.118	1.663 ± 0.209	0.067 ± 0.007	3.763 ± 0.193
10 mg/kg	4.833 ± 0.269	1.864 ± 0.083	0.088 ± 0.006	4.574 ± 0.090
15 mg/kg	5.631 ± 0.267[a]	1.765 ± 0.142	0.169 ± 0.013[a]	4.570 ± 0.222

[a]Represents a significant difference compared with the control group (p < 0.05), n = 5.

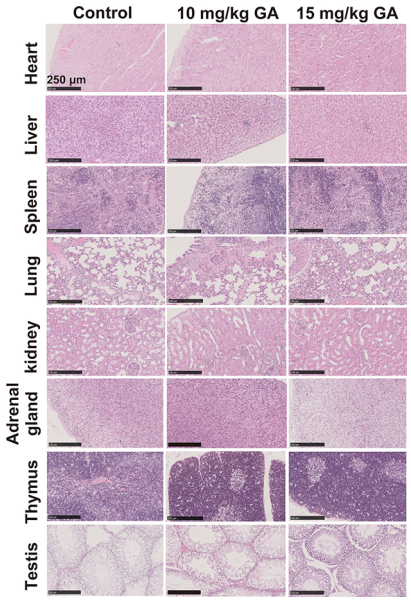

Figure 2. Effect of GA ($Au_{29}SG_{27}$ cluster) on histology of organs in rats after 30 days of intraperitoneal injection. Representative histopathological images of main organs from the rats treated with vehicle (saline), 10 mg Au/kg of GA, and 15 mg Au/kg of GA on day 30 (n = 5 per group, HE staining; scale bars = 250 μm).

induce slight toxicity to normal rats, especially considering some hematological index and organ coefficients, while 10 mg Au/kg of GA did not cause any unexpected side effects.

Dose-Dependent Therapeutic Effect of GA in Collagen-Induced Arthritis Model. To determine the optimal dose of GA for RA therapy in rats, a collagen-induced arthritis (CIA) model, the most commonly used model for RA therapeutic evaluation, was used in this study.[20,21] On the basis of the 30-day toxicity assessment of the Au cluster, we chose 0.5 mg Au/kg (1/20 of 10 mg Au/kg) as the initial treatment dose and then gradiently increased to 5 mg Au/kg per day. After the RA model was completely established (day 22 post primary collagen immunization), rats were injected every day with 0.5−5 mg Au/kg of GA (0.5, 1, 2.5, and 5 mg Au/kg) for 42 days and compared with saline-treated CIA rats. Non-immunized rats injected intraperitoneally with an equal volume of saline were served as the normal control. The change of body weight in each group was monitored during the whole course of treatment. Data revealed that CIA decreased the body weight of normal rats, but GA treatment did not further aggravate this reduction in all dose groups (Figure 3A). During the test, swelling of the joints was assessed by measuring the ankle circumference of each rat every week, and the clinic arthritis index was scored (0−4 point) according to clinical observation. Statistics on mean ankle circumference suggest that the swelling of the joints was induced by CIA and sustained for the whole time after the model was established (Figure 3B). Among the GA-treated groups, only the dose of 5 mg Au/kg significantly alleviated the swelling from the fourth week, while other low doses slightly improved symptoms without statistical significance (Figure 3B). The clinical score on arthritis showed similar results to the mean ankle circumference evaluation. Only 5 mg Au/kg of GA significantly remitted the swelling and tenderness compared with the model group from the third week (Figure 3C). Other low doses of GA did not significantly improve the clinical symptoms of arthritis (Figure 3C). Representative photographs of the hind claws of each group at the beginning, middle, and end of administration were shown in Figure 3D, which provides visible evidence for the therapeutic effect of GA.

Dose-Dependent Efficacy of GA on Inflammation Suppression in CIA Rats. Subsequently, histopathological sections of hind claws were assessed after the rats were sacrificed to evaluate the inflammation within periarticular soft tissues and synovial tissues. Histopathological observation

DOI: 10.1021/acsomega.9b02003
ACS Omega 2019, 4, 14092−14099

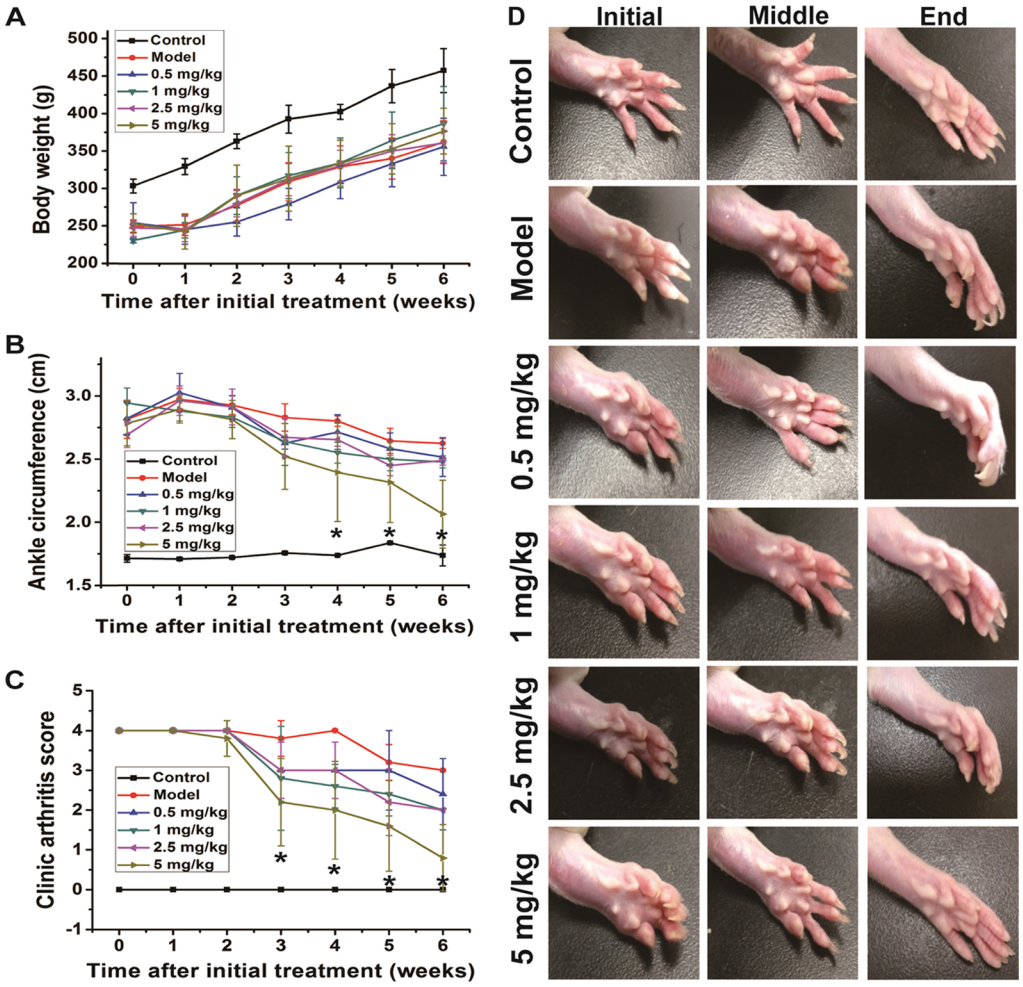

Figure 3. Dose-dependent therapeutic effect of GA in CIA rats. (A) Changes of body weight in CIA rats during 6 weeks of treatment with vehicle (saline) and 0.5, 1, 2.5, and 5 mg Au/kg of GA. Non-immunized rats treated with vehicle were used as a control group. Data are presented as mean ± SD; $n = 5$ per group. (B) Progression of ankle circumference in CIA rats during 6 weeks of treatment. $n = 5$ per group; $^*p < 0.05$ compared to the vehicle-treated group (Model). (C) Progression of clinical arthritis score in CIA rats during 6 weeks of treatment. $n = 5$; $^*p < 0.05$ compared to the vehicle-treated group (Model). (D) Representative photographs of CIA rats treated with vehicle (Model) and 0.5, 1, 2.5, and 5 mg Au/kg of GA at the initial, middle, and end time points of treatment.

indicated that CIA induced obvious synovium hyperplasia and inflammatory cell infiltration around the rheumatic joints (Figure 4A). Both 2.5 and 5 mg Au/kg of GA can attenuate the synovial inflammation effectively, but not the lower doses (Figure 4A). Statistics of histology score supported the observation judgment that 2.5 mg Au/kg ($p < 0.05$) and 5 mg Au/kg ($p < 0.01$) of GA significantly suppress the CIA-induced synovial inflammation, while the lower doses did not (Figure 4B). The chronic inflammation of RA was mainly conducted by sustained high levels of proinflammatory factors, including TNF-α, IL-1β, and IL-6. The effect of GA on these biochemical parameters in the serum of CIA rats was determined by radioimmunoassay. Results showed that CIA increased all of these cytokines in serum, while GA treatments reduced this increase in a dose-dependent manner (Figure 4C). According to the significant examination, only 2.5 mg Au/kg ($p < 0.05$) and 5 mg Au/kg ($p < 0.01$) of GA could significantly inhibit the upregulation of all three proinflammatory factors, which is consistent with the histopathological observation.

Dose-Dependent Efficacy of GA on Bone Destruction Prevention in CIA Rats. The most deleterious effect caused by RA is bone erosion in joints. The effect of GA on the progression of cartilage/bone destruction was evaluated by histopathological analysis and microCT scan on the ends of metatarsal. Histopathological observations within joints showed that the CIA model induces serious damage in both cartilage and bone, while the higher doses of GA treatment could attenuate the erosion obviously (Figure 4A). Histological score analysis of cartilage and bone damage showed that exceeding 1 mg Au/kg of GA could significantly prevent CIA-induced cartilage/bone erosion in a dose-dependent manner (Figure 4B). Results of microCT analysis also revealed that CIA induced very serious damage to articular bones and caused many bone resorption pits and holes in joints, while higher doses of GA treatment could effectively attenuate this destruction (Figure 5A). Most noteworthy, the 5 mg Au/kg GA treatment almost restored the bone damage to the normal state, while the lower dose groups still had some erosion pits (Figure 5A). Bone mineral density (BMD) analysis, consistent with the microCT observations, showed that only 5 mg Au/kg of GA can attenuate the CIA-induced bone loss to a significant extent.

DOI: 10.1021/acsomega.9b02003
ACS Omega 2019, 4, 14092−14099

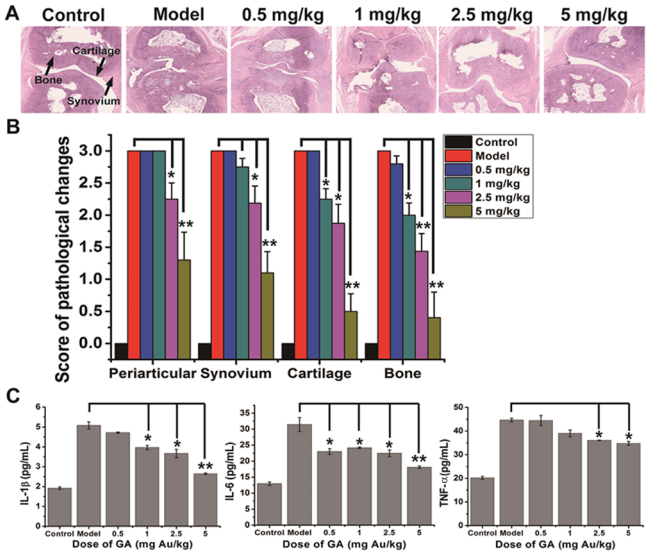

Figure 4. Dose-dependent efficacy of GA on inflammation suppression in CIA rats. (A) Representative histopathological photos of joint sections from normal control rats and CIA rats treated with vehicle (saline) and 0.5, 1, 2.5, and 5 mg Au/kg of GA at the end of the 42-day treatment. The synovium, cartilage, and bone were indicated by black arrows. (B) Histological scores of inflammation in periarticular and synovium as well as cartilage/bone destruction in CIA rats treated with vehicle and 0.5, 1, 2.5, and 5 mg Au/kg of GA on day 42 of treatment. The non-immunized rats were used as controls. Data are presented as mean ± SD; n = 5 per group; *p < 0.05, **p < 0.01 compared to the vehicle-treated group (Model). (C) Levels of pro-inflammatory cytokines (TNF-α, IL-1β, and IL-6) in the serum of CIA mice treated with vehicle and 0.5, 1, 2.5, and 5 mg Au/kg of GA at the end of the 42-day treatment. The non-immunized rats were used as controls. Data are presented as mean ± SD; n = 5 per group; *p < 0.05, **p < 0.01 compared to the vehicle-treated group (Model).

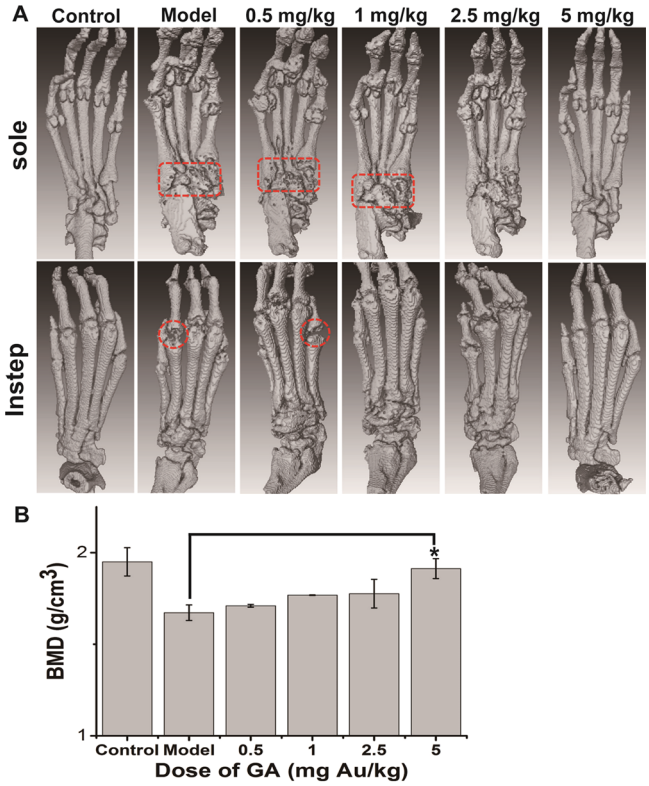

Figure 5. Dose-dependent efficacy of GA on bone destruction prevention in CIA rats: (A) Representative images of microCT observation in each group (n = 5 per group) of CIA mice treated with vehicle and 0.5, 1, 2.5, and 5 mg Au/kg of GA and normal control group at the end of the 42-day treatment. The typical site of severe bone erosion is marked by the dotted box (pit) and dotted circle (cavity). (B) Bone mineral density (BMD) analysis of the microCT scan in each group (n = 5 per group). Data are presented as mean ± SD; *p < 0.05 compared to the vehicle-treated group (Model).

At the end of treatments, histopathological changes in the main organs of CIA rats were examined to determine whether any damage was induced by GA treatment. The observation indicated that the 42-day continuous administration of GA did not induce any noticeable damage to organs in CIA rats at these doses (Figure 6). These results suggested that, considering the anti-inflammatory and osteoprotective activity as well as the biosafety in the treatment of RA, 5 mg Au/kg of GA is the optimal dose in rats.

DISCUSSION

Rheumatoid arthritis (RA) is characterized by the presence of inflammatory synovitis and progressive cartilage/bone destruction, but the pathogenesis is still not completely understood.[1] Joint destruction is the most severe outcome of this disease and the major cause of disability.[3] Conventional DMARDs usually aim to inhibit the inflammation, and very few treatments aim to improve RA-associated bone loss.[3,20] Although the prospects for most patients are currently favorable, a large number of patients are still suffering from severe dysfunction in arthritic joints.[1] Among conventional DMARDs, gold drugs appear to be very potent inhibitors of inflammation and showed some potential influences on bone metabolism *in vitro*.[6,8] However, the serious side effects of gold drugs lead to a decline of clinical applications in recent years.[5,22] Therefore, more research is needed to develop

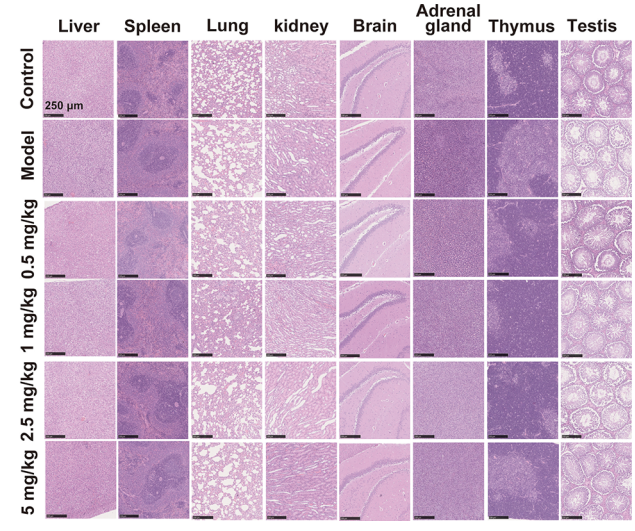

Figure 6. Effect of GA treatment on organ histology of CIA rats intraperitoneally administrated for 6 weeks. Representative histopathological images of main organs from the rats treated with vehicle and 0.5, 1, 2.5, and 5 mg Au/kg of GA and normal control group at the end of the 42-day treatment (n = 5 per group, HE staining; scale bars = 250 μm).

DOI: 10.1021/acsomega.9b02003
ACS Omega 2019, 4, 14092−14099

innovative gold drugs, which not only retain the activity of chrysotherapy but also have minimal side effects.

In recent years, several studies have reported that non-modified gold nanoparticles exhibit potential RA therapeutic activity in CIA rats without serious toxicity and side effects.[23−26] For example, prophylactic intra-articular treatment with 13 or 50 nM gold nanoparticles in the early stage of arthritis can significantly inhibit joint swelling and cartilage erosion.[23,26] In established arthritis of rats, continuous intra-articular treatment of these two nanoparticles can also effectively ameliorate the symptoms.[24] However, this local injection is not conducive to a comprehensive assessment of its biosafety. In another study, continuous intraperitoneal injection of gold particles about 15 nM in diameter showed effective anti-arthritis activity in CIA rat models, but its biosafety was not assessed in this study.[25] In addition, the mechanisms of the anti-arthritis activity of these gold nanoparticles are still not very clear. In these studies, the beneficial response of gold nanoparticles was attributed to the suppression of inflammatory mediators and inhibition of VEGF (vascular endothelial growth factor) or antioxidant properties.[23−26]

As novel gold nanomaterials, gold clusters synthesized with biomolecules (especially for peptides) have attracted much attention for their excellent biocompatibilities and synergistic biomedical properties.[11,12] We have prepared a Au cluster composed of 29 gold atoms and 27 GSH peptides in each molecule, named GA ($Au_{29}SG_{27}$).[16] The LD_{50} of GA injected intraperitoneally in SD rats was nearly 39 times higher than that of auranofin.[7,16] In a previous study, we found that the gold cluster could markedly inhibit RANKL-mediated osteoclastogenesis and LPS-induced proinflammatory secretion *in vitro* and attenuate arthritis and bone destruction in a CIA rat model.[16] In CIA rats, the cluster exhibits similar anti-inflammatory activity to methotrexate, the first-line clinical anchored antirheumatic drug, and is superior to methotrexate in preventing cartilage/bone destruction.[16,27] Therefore, peptide-protected gold clusters have shown fine therapeutic activity for RA in preclinical studies and revealed great potential for future clinical applications.

The efficacy and safety of drugs are closely related to dosage, which is a very crucial issue in clinical transformation research.[19,28] Therefore, the dose-dependent efficacy of the GA cluster on RA therapy and biosafety was comprehensively assessed in this study. We found that continuous intraperitoneal administration of 20 mg Au/kg of GA resulted in individual animal death, but 15 and 10 mg Au/kg did not. However, compared with saline-treated rats, 15 mg Au/kg of GA induced several changes in hematological parameters (Gran%, HCT, Mid%, MCHC, and PCT) and organ coefficients (kidney and adrenal gland) during a 30-day toxicity assessment, while 10 mg Au/kg of GA did not induce any significant toxicity and side effects. Despite the slight increase in renal organ index induced by 15 mg Au/kg of GA, no obvious pathological damage was observed from histopathology observations. Considering the tissue distribution of Au after the GA treatment reported previously, gold is highly distributed in the kidney.[16] Therefore, we speculate that this phenomenon is caused by the accumulation of gold. These data indicate that the continuous administration of GA at doses below 10 mg Au/kg will be safe *in vivo* of rats. Then, we evaluated the therapeutic effects of a series of doses of GA in a rat RA model, including 0.5, 1, 2.5, and 5 mg Au/kg, to determine the lowest dose that can significantly suppress both inflammation and bone damage. Results showed that there is a dose-dependent therapeutic effect of GA in this range. Assessments on joint circumference and clinic arthritis score showed that only 5 mg Au/kg of GA could significantly improve RA symptoms. This conclusion was further proved by histopathological examination and microCT analysis. These data showed that 1 mg Au/kg of GA can significantly inhibit inflammation but not obviously suppress cartilage/bone destruction. Although 2.5 mg Au/kg of GA could significantly suppress both inflammation and bone damage, only 5 mg Au/kg of GA could restore the joint state to near normal control. Detection of proinflammatory factors in the serum also showed that 5 mg Au/kg of GA had the highest activity in suppressing inflammation. A previous study proved that the bone destruction in RA was initiated by several pro-inflammatory cytokines produced by macrophages, such as TNF-α and IL-1β.[29] These cytokines increase the expression of receptor activator of nuclear factor κB ligand (RANKL) to promote the differentiation of bone-resorbing osteoclasts.[6,30] In a previous study, we found that the gold clusters not only inhibited the overexpression of LPS-induced pro-inflammatory cytokines in macrophages but also directly inhibited the differentiation of osteoclasts induced by RANKL *in vitro*.[16] In this study, lower doses of GA showed significant improvement in bone damage, but not in inflammation suppression, such as the dose of 1 mg Au/kg. These results suggest that GA not only protects the bone by inhibiting inflammation but also plays a direct role in preventing bone destruction. Furthermore, 5 mg Au/kg GA treatment for 42 days did not induce a significant influence on the gain of body weight and the histopathology of main organs in CIA rats, which indicated its high biosafety. Therefore, we conclude that the dose of 5 mg Au/kg is the optimal dose of GA for RA therapy in rats. We hope that this study could facilitate the clinical transformation of such active gold clusters in the near future.

MATERIALS AND METHODS

Materials. Glutathione (GSH = γ-Glu-Cys-Gly) and $HAuCl_4{\cdot}3H_2O$ were purchased from Sigma-Aldrich (USA). Bovine type II collagen and incomplete Freund's adjuvant were purchased from Chondrex, Inc. (USA). All Sprague−Dawley (SD) rats were purchased from Hua Fukang Biotechnology Co., Ltd. (Beijing, China). Deionized water of Milli-Q purity grade (18.2 MΩ·cm) was obtained with a Milli-Q water system (USA).

Synthesis and Characterization of $Au_{29}SG_{27}$ Clusters. The $Au_{29}SG_{27}$ clusters were synthesized and purified according to a previously reported method.[16,31] In brief, an equal volume of freshly prepared 30 mM GSH aqueous solution and 20 mM HAuCl4 aqueous solution were mixed under gentle stirring (500 rpm) for 10 min at 25 °C. Next, the reaction mixture was heated to 70 °C for 12 h under mild stirring (500 rpm) and then kept at room temperature for another 12 h in the dark. Subsequently, the reaction mixture was centrifuged at 10,000 rpm for 30 min to remove the precipitated large particles and then purified by adding a 3-fold volume of ethanol to the as-synthesized clusters. The solution was fully mixed and centrifuged at 10,000 rpm for 15 min to discard the supernatant containing free GSH and gold ions. Retained precipitation was washed three times with 75% ethanol. Purified clusters were re-dissolved in ultrapure water with the assistance of sodium hydroxide. The solution was centrifuged

DOI: 10.1021/acsomega.9b02003
ACS Omega 2019, 4, 14092−14099

at 10,000 rpm for 30 min to remove the insoluble components. The cluster solution was further purified using an ultrafiltration tube (Millipore, MWCO: 3 kDa) to remove the free ions. The fluorescence spectrum of purified clusters was detected to verify the products by using an RF-5301 fluorescence spectrophotometer (Shimadzu, Japan). An aliquot of purified cluster was detected by inductively coupled plasma mass spectrometry (Thermo Elemental X7) to quantify the Au content, and the rest was sealed and stored in the dark at 4 °C.

Toxicity Assessment. Twenty male SD rats with an average body weight of 200 g were randomly assigned to four groups, each consisting of five animals: control group, saline injected; low dose group, 10 mg Au/kg of GA injected; medium dose group, 15 mg Au/kg of GA injected; and high dose group, 20 mg Au/kg of GA injected. All groups were intraperitoneally injected with corresponding drugs every 2 days for 30 days. The rats were given food and water freely during the experimental procedures. The body weight of each mouse was closely monitored every week. At the end of the treatment, blood sample was collected from each rat for hematological and biochemical analyses. The major organs, including heart, liver, spleen, lung, kidney, testis, adrenal gland, and thymus, were harvested after the rats were sacrificed and weighed following their dissection. Then, these organs were fixed in 10% neutral buffered formalin, embedded into paraffin routinely, and sectioned to 8 μm slices. The obtained slices were stained for histopathological examination by using hematoxylin and eosin (HE) and analyzed under a microscope. All animal care and experiments were approved by the Institutional Animal Care and Ethic Committee at the Chinese Academy of Sciences (approved no. SYXK (jing) 2014-0023).

Collagen-Induced Arthritis (CIA) Model and Treatment Protocols. All animal care and experiments were approved by the Institutional Animal Care and Ethic Committee at the Chinese Academy of Sciences (approved no. SYXK (jing) 2014-0023) and carried out in accordance with the National Act on the use of experimental animals (China). Native bovine type II collagen was dissolved in 0.1 mM acetic acid at 4 °C overnight, and the immune emulsion (2 mg/mL) was prepared by emulsifying with an equal volume of Complete Freund's Adjuvant. Five- to 6-week-old SD male rats (180−200 g) were subcutaneously injected at the base of the tail with 0.2 mL of the emulsion containing 400 μg of type II collagen. Seven days after the primary immunization, rats were boosted subcutaneously with 200 μg of type II collagen immune emulsion once again. Rats were closely monitored for arthritis disease progression by assessing ankle circumference and clinical arthritis score. The clinical arthritis score of each paw was assessed by using semiquantitative scoring of five grades (0−4) according to the degree of erythema and swelling: 0 = no erythema or swelling; 1 = slight erythema or swelling of one toe or finger; 2 = erythema and swelling on more than one toe or finger; 3 = erythema and swelling of ankle or wrist; and 4 = complete erythema and swelling of toes or fingers and ankles or wrists.[32] Every claw was graded, and a mean score was calculated for each animal. At day 21 after the first immunization, the rats with clinical scores of 3 and 4 were randomly assigned to five groups to initiate the treatment, each group contained five rats: group I, saline-treated CIA rats; group II, CIA rats treated with 0.5 mg Au/kg/day of GA; group III, CIA rats treated with 1 mg Au/kg/day of GA; group IV, CIA rats treated with 2.5 mg Au/kg/day of GA; and group V, CIA rats treated with 5 mg Au/kg/day of GA. Five saline-treated non-immunized rats served as a normal control. Saline and GA dissolved in saline were intraperitoneally injected once a day and continuously administered for 6 weeks (42 days). During the treatment period, ankle circumference and clinical arthritis score as well as the body weight of each rat were measured every week. At the end of the treatment, blood sample of each rat was collected and centrifuged to obtain the serum for conducting proinflammatory cytokine detection. The concentrations of TNF-α, IL-1β, and IL-6 in the serum were determined by radioimmunoassay in Fraser Biotechnology Co., Ltd. (Beijing, China). Then, rats were sacrificed by excess CO2 inhalation, and the hind limbs of each rat were harvested for three-dimensional microfocus computed tomography (microCT) analysis and histopathological examination. The major organs including the brain, liver, spleen, lung, kidney, testis, adrenal gland, and thymus were dissected and fixed in 10% neutral buffered formalin for histopathological examination.

MicroCT Analyses and Histopathological Analysis. The hind limb of each rat was harvested after sacrifice and analyzed with microCT (IVIS Spectrum CT, Perkin Elmer, USA) at a voltage of 90 kV and an electric current of 88 μA. The scan mode is high resolution, and the scanning resolution is about 72 μM. The bone mineral density (BMD) was analyzed using AccuCT software (Perkin Elmer, USA). For histopathological analysis, hind paws were fixed in 10% neutral buffered formalin and decalcified in 5% formic acid, embedded in paraffin, sectioned to ∼5 μm-thick slices, and stained with hematoxylin and eosin. Histopathological changes in periarticular tissue, synovium, cartilage, and bone were described and scored by using semiquantitative scoring of four grades (0−3) according to the severity. Major organs were also isolated and fixed in 10% neutral buffered formalin, embedded in paraffin, sectioned to 5 μm-thick slices, and stained with HE for histopathological examination.

Statistical Analyses. Statistical analysis was carried out by using SPSS 16.0 software (SPSS, USA). Data are described as mean ± standard deviation (SD). Data were first tested for homogeneity of variance by using Levene's test. Statistical significance of overall differences between multiple groups was assessed by one-way ANOVA, and $p < 0.05$ was regarded as significant.

AUTHOR INFORMATION

Corresponding Authors

*E-mail: gaoxy@ihep.ac.cn. Tel: 86-10-88236709. (X.G.).
*E-mail: gaofp@ihep.ac.cn (F.G.).

ORCID

Fuping Gao: 0000-0002-0287-9763
Jinsong Zhang: 0000-0003-2032-1111
Xueyun Gao: 0000-0002-2267-9945

Author Contributions

⊥Q.Y. and Y.Z. have equal contribution to the work.

Notes

The authors declare no competing financial interest.

ACKNOWLEDGMENTS

This work was supported by the National Natural Science Foundation of China (21425522, 21727817, 11621505, 31700874, and 31670976), Beijing Science and Technology Commission Special Project for Frontier Technology in Life

DOI: 10.1021/acsomega.9b02003
ACS Omega 2019, 4, 14092−14099

Sciences (Z171100000417008), and Beijing Municipal High Level Innovative Team Building Program (IDHT20180504).

REFERENCES

(1) Smolen, J. S.; Aletaha, D.; McInnes, I. B. Rheumatoid arthritis. *Lancet* **2016**, *388*, 2023−2038.
(2) Firestein, G. S. Evolving concepts of rheumatoid arthritis. *Nature* **2003**, *423*, 356−61.
(3) Findlay, D. M.; Haynes, D. R. Mechanisms of bone loss in rheumatoid arthritis. *Mod. Rheumatol.* **2005**, *15*, 232−240.
(4) Kikuta, J.; Ishii, M. Osteoclast migration, differentiation and function: novel therapeutic targets for rheumatic diseases. *Rheumatol.* **2013**, *52*, 226−234.
(5) Eisler, R. Chrysotherapy: a synoptic review. *Inflammation Res.* **2003**, *52*, 487−501.
(6) Bondeson, J. The mechanisms of action of disease-modifying antirheumatic drugs: a review with emphasis on macrophage signal transduction and the induction of proinflammatory cytokines. *Gen. Pharmacol.* **1997**, *29*, 127−150.
(7) Kean, W. F.; Hart, L.; Buchanan, W. W. Auranofin. *Br. J. Rheumatol.* **1997**, *36*, 560−572.
(8) Hall, T. J.; Jeker, H.; Nyugen, H.; Schaeublin, M. Gold salts inhibit osteoclastic bone resorption in vitro. *Inflammation Res.* **1996**, *45*, 230−233.
(9) Felson, D. T.; Anderson, J. J.; Meenan, R. F. The comparative efficacy and toxicity of second-line drugs in rheumatoid arthritis. Results of two metaanalyses. *Arthritis Rheum.* **1990**, *33*, 1449−1461.
(10) Felson, D. T.; Anderson, J. J.; Meenan, R. F. Use of short-term efficacy/toxicity tradeoffs to select second-line drugs in rheumatoid arthritis. A metaanalysis of published clinical trials. *Arthritis Rheum.* **1992**, *35*, 1117−1125.
(11) Yuan, Q.; Wang, Y.; Zhao, L.; Liu, R.; Gao, F.; Gao, L.; Gao, X. Peptide protected gold clusters: chemical synthesis and biomedical applications. *Nanoscale* **2016**, *8*, 12095−12104.
(12) Luo, Z.; Zheng, K.; Xie, J. Engineering ultrasmall water-soluble gold and silver nanoclusters for biomedical applications. *Chem. Commun.* **2014**, *50*, 5143−5155.
(13) Yao, Q.; Chen, T.; Yuan, X.; Xie, J. Toward Total Synthesis of Thiolate-Protected Metal Nanoclusters. *Acc. Chem. Res.* **2018**, *51*, 1338−1348.
(14) Zheng, K.; Setyawati, M. I.; Leong, D. T.; Xie, J. Antimicrobial Gold Nanoclusters. *ACS Nano* **2017**, *11*, 6904−6910.
(15) Thakor, A. S.; Jokerst, J.; Zavaleta, C.; Massoud, T. F.; Gambhir, S. S. Gold Nanoparticles: A Revival in Precious Metal Administration to Patients. *Nano Lett.* **2011**, *11*, 4029−4036.
(16) Gao, F.; Yuan, Q.; Cai, P.; Gao, L.; Zhao, L.; Liu, M.; Yao, Y.; Chai, Z.; Gao, X. Au Clusters Treat Rheumatoid Arthritis with Uniquely Reversing Cartilage/Bone Destruction. *Adv. Sci.* **2019**, *6*, 1801671.
(17) Yuan, Q.; Gao, F.; Yao, Y.; Cai, P.; Zhang, X.; Yuan, J.; Hou, K.; Gao, L.; Ren, X.; Gao, X. Gold Clusters Prevent Inflammation-Induced Bone Erosion through Inhibiting the Activation of NF-κB Pathway. *Theranostics* **2019**, *9*, 1825−1836.
(18) Carnovale, C.; Bryant, G.; Shukla, R.; Bansal, V. Identifying Trends in Gold Nanoparticle Toxicity and Uptake: Size, Shape, Capping Ligand, and Biological Corona. *ACS omega* **2019**, *4*, 242−256.
(19) Paradossi, G.; Oddo, L.; Cerroni, B.; Ben-Harush, C.; Ariel, E.; Di Meco, F.; Ram, Z.; Grossman, R. In Vivo Toxicity Study of Engineered Lipid Microbubbles in Rodents. *ACS omega* **2019**, *4*, 5526−5533.
(20) Cantley, M. D.; Smith, M. D.; Haynes, D. R. Pathogenic bone loss in rheumatoid arthritis: Mechanisms and therapeutic approaches. *Int. J. Clin. Rheumatol.* **2009**, *4*, 561−582.
(21) Staines, N. A.; Wooley, P. H. Collagen arthritis–what can it teach us? *Br. J. Rheumatol.* **1994**, *33*, 798−807.
(22) Messori, L.; Marcon, G. Gold complexes in the treatment of rheumatoid arthritis. *Met. Ions Biol. Syst.* **2004**, *41*, 279−304.
(23) Tsai, C. Y.; Shiau, A. L.; Chen, S. Y.; Chen, Y. H.; Cheng, P. C.; Chang, M. Y.; Chen, D. H.; Chou, C. H.; Wang, C. R.; Wu, C. L. Amelioration of collagen-induced arthritis in rats by nanogold. *Arthritis Rheum.* **2007**, *56*, 544−554.
(24) Leonavičiene, L.; Kirdaitė, G.; Bradūnaitė, R.; Vaitkienė, D.; Vasiliauskas, A.; Zabulytė, D.; Ramanavičienė, A.; Ramanavicius, A.; Ašmenavičius, T.; Mackiewicz, Z. Effect of Gold Nanoparticles in the Treatment of Established Collagen Arthritis in Rats. *Medicina* **2012**, *48*, 16.
(25) Khan, M. A.; Khan, M. J. Nano-gold displayed anti-inflammatory property via NF-kB pathways by suppressing COX-2 activity. *Artif. Cells, Nanomed., Biotechnol.* **2018**, *46*, 1149−1158.
(26) Kirdaite, G.; Leonaviciene, L.; Bradunaite, R.; Vasiliauskas, A.; Rudys, R.; Ramanaviciene, A.; Mackiewicz, Z. Antioxidant effects of gold nanoparticles on early stage of collagen-induced arthritis in rats. *Res. Vet. Sci.* **2019**, *124*, 32−37.
(27) Smolen, J. S.; Landewe, R.; Bijlsma, J.; Burmester, G.; Chatzidionysiou, K.; Dougados, M.; Nam, J.; Ramiro, S.; Voshaar, M.; van Vollenhoven, R.; Aletaha, D.; Aringer, M.; Boers, M.; Buckley, C. D.; Buttgereit, F.; Bykerk, V.; Cardiel, M.; Combe, B.; Cutolo, M.; van Eijk-Hustings, Y.; Emery, P.; Finckh, A.; Gabay, C.; Gomez-Reino, J.; Gossec, L.; Gottenberg, J. E.; Hazes, J. M. W.; Huizinga, T.; Jani, M.; Karateev, D.; Kouloumas, M.; Kvien, T.; Li, Z.; Mariette, X.; McInnes, I.; Mysler, E.; Nash, P.; Pavelka, K.; Poor, G.; Richez, C.; van Riel, P.; Rubbert-Roth, A.; Saag, K.; da Silva, J.; Stamm, T.; Takeuchi, T.; Westhovens, R.; de Wit, M.; van der Heijde, D. EULAR recommendations for the management of rheumatoid arthritis with synthetic and biological disease-modifying antirheumatic drugs: 2016 update. *Ann. Rheum. Dis.* **2017**, *76*, 960−977.
(28) Mei, L.; Zhang, X.; Yin, W.; Dong, X.; Guo, Z.; Fu, W.; Su, C.; Gu, Z.; Zhao, Y. Translocation, biotransformation-related degradation, and toxicity assessment of polyvinylpyrrolidone-modified 2H-phase nano-MoS_2. *Nanoscale* **2019**, *11*, 4767−4780.
(29) Feldmann, M.; Brennan, F. M.; Foxwell, B. M.; Maini, R. N. The role of TNF alpha and IL-1 in rheumatoid arthritis. *Curr. Dir. Autoimmun.* **2001**, *3*, 188−199.
(30) Boyle, W. J.; Simonet, W. S.; Lacey, D. L. Osteoclast differentiation and activation. *Nature* **2003**, *423*, 337.
(31) Luo, Z.; Yuan, X.; Yu, Y.; Zhang, Q.; Leong, D. T.; Lee, J. Y.; Xie, J. From Aggregation-Induced Emission of Au(I)-Thiolate Complexes to Ultrabright Au(0)@Au(I)-Thiolate Core-Shell Nanoclusters. *J. Am. Chem. Soc.* **2012**, *134*, 16662−16670.
(32) Mauri, C.; Mars, L. T.; Londei, M. Therapeutic activity of agonistic monoclonal antibodies against CD40 in a chronic autoimmune inflammatory process. *Nat. Med.* **2000**, *6*, 673−679.

DOI: 10.1021/acsomega.9b02003
ACS Omega 2019, 4, 14092−14099